A High-Resolution X-Ray Microscope for Laser-Driven Planar-Foil Experiments

A soft x-ray microscope ($E \lesssim 3$ keV) with high spatial resolution (~3 μm) has been characterized at LLE and used for initial experiments on the OMEGA laser system to study the hydrodynamic stability of directly driven planar foils. The microscope, which is an optimized Kirkpatrick-Baez (KB)–type design, is used to obtain four x-ray radiographs of laser-driven foils. Time-resolved images are obtained with either custom-built framing cameras (time resolution ~80 ps) or short-pulse backlighter beams ($\Delta t \lesssim 200$ ps). In the former case, a spatial resolution of ~7 μm was obtained (limited by the framing camera), while in the latter case a resolution of ~3 μm was obtained. This article details the testing, calibration, and initial use of this microscope in the laboratory and on OMEGA.

Recent experiments studying the hydrodynamic stability of laser-driven planar foils[1–7] have relied on the technique of time-resolved x-ray radiography as a method of diagnosis. The short time scales (~ ns) require the use of a laser-generated x-ray backlighter, while the small spatial scale lengths (~ μm) require a high-spatial-resolution imaging system. In a radiograph of a perturbed driven foil undergoing unstable growth, the modulation depth (the desired observable) is affected by the resolution (modulation transfer function) of the imaging system.[8] This is typically limited by the imaging system itself (pinhole resolution in the case of pinhole imaging) or additionally by the recording system blurring (as is typically the case when using framing camera or streak camera imaging). Systems used to record radiographs of laser-driven foils range from simple pinhole cameras coupled to x-ray framing cameras to Wolter microscopes coupled to streak cameras. A good example of the resolution obtainable with a pinhole–framing camera combination is described in Robey *et al.*,[9] where 5- to 10-μm-diam pinholes in combination with framing cameras at magnifications up to 12× yield a spatial resolution approaching 10 μm. Remington *et al.*[10] describe the measured resolution of the Nova 22× Wolter microscope, which has an ultimate resolution of ~2 to 3 μm but is not easily adaptable to multiple-frame, two-dimensional imaging. More recently, monochromatic imaging using bent crystals as the imaging device has been applied to flat-foil experiments.[7] Resolution approaching ~3 μm has been reported. Kodama *et al.*[11] report on an advanced Kirkpatrick–Baez (AKB) microscope, which consists of four mirrors producing a single image. This microscope has a quoted resolution of ~3 μm or better over an ~1-mm-diam region.

This work describes the characterization of a KB microscope configured to provide high-spatial-resolution (~3-μm), low-energy (≲3-keV), multiple framed images (Δt ~ 80 ps) of x-ray-backlit, laser-driven foils. This KB microscope optical assembly consists of glass reflecting surfaces assembled without an additional metal coating. As will be shown below, the uncoated reflecting surfaces provide a convenient high-energy cutoff at ~3 keV, which is appropriate to both the backlighter spectrum and the subjects of the radiography (plastic foils). The detailed design is further described in Marshall and Su.[12] Time resolution can be obtained by either custom framing cameras (developed at the Los Alamos National Laboratory[13]) or a novel, multibeam, short-pulse (~100-ps) backlighter irradiation scheme. This KB microscope will be used in future planar-foil stability experiments on the University of Rochester's OMEGA laser system.[14]

Characterization of the Microscope

The microscope used for these experiments was built and assembled by Sydor Optics.[15] It consists of four mirrors arranged in a stack of two perpendicular pairs (Fig. 74.27) that produce four images of laser–plasma x-ray emission. Images are formed by two perpendicular reflections at a mean grazing angle of ~0.70°. The super-polished reflecting surfaces (surface roughness < 4 Å) are concave with radii of curvature r = 26 m and a thickness along the optical axis of 4.5 mm. [Previously reported mirror assemblies (Ref. 12) had a thickness of 9 mm, resulting in a larger solid angle but also larger measured and calculated off-axis aberrations.] The surfaces perpendicular to the reflecting surfaces are also super polished and are used to optically contact the mirrors into a fixed, stable assembly. The images formed by the KB microscope obey the focus equation[16]

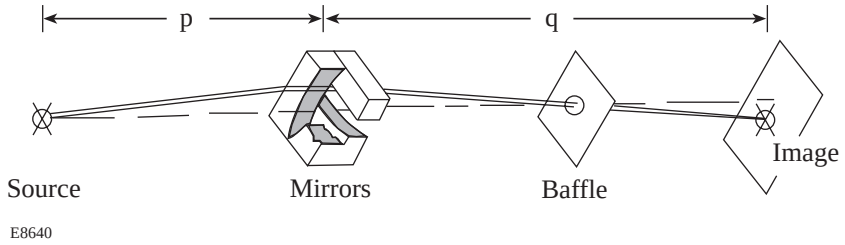

Figure 74.27
Schematic of the KB microscope optical assembly.

$$\frac{1}{p}+\frac{1}{q}=\frac{2}{R\sin i}, \tag{1}$$

where p is the distance from the object to the mirror assembly, q is the distance from the mirror assembly to the image, i is the grazing angle, and R is the radius of curvature of the mirrors. The distances p and q in Eq. (1) refer to the distance from the center of the assembly, i.e., between the pairs of perpendicular mirrors. The mirror separations have been adjusted (as described in Ref. 12) so that the focus of the first reflecting surface is coincident with the second reflecting surface. The best-focus distance at a magnification of 13.6 was found to be p = 179.3 mm. The solid angle subtended by each reflecting pair as seen from the source is $\sim 9\times 10^{-8}$ sr for this case.

After assembly the KB microscope was first characterized in the laboratory using a cw, e-beam-generated x-ray source. The e-beam impinged on a water-cooled tungsten target after passing through a bending magnet whose purpose was to prevent ion contamination of the target area. Typical e-beam voltage settings of 10 kV were used in all tests, producing a continuum x-ray source up to 10 keV. Images were recorded on Kodak DEF direct-exposure film after passing through a 1-mil (25.4-μm) Be window placed near the optic baffle. Figure 74.28(a) shows one of four such images taken of a 500-mesh Cu grid (0.001-in.-diam Cu wires spaced by 0.002 in., i.e., 500/in.) placed at the best focus of the microscope. A hole was placed in the grid [visible in Fig. 74.28(a) as a dark irregularly shaped region] as a position reference from image to image. The resolution as a function of position was determined from photomicrodensitometer (PDS)-digitized grid images. A Perkin–Elmer PDS with a 0.25 NA lens, and a scanning aperture of 10 μm, was used to digitize the images. Figure 74.28(b) shows a horizontal lineout through the image of Fig. 74.28(a) and just below the reference hole. The values are computed intensity in ergs/cm^2 versus position in μm [assuming a photon energy of 2 keV (see the energy response calibration later in this section) and using the semi-empirical formula of Henke *et al.*[17]]. The lineout has been averaged over the width of the space between the wires and median filtered to reduce point-to-point noise. The remaining pattern shows the overall resolution of the image near best focus. Figure 74.28(c) shows an enlargement of the lineout at the edge of the shadow of one wire. The width of the shadow is ~3.7 μm. This measurement was repeated across the image, yielding the resolution as a function of position [Fig. 74.28(d)]. The resolution thus measured closely follows that computed by ray tracing (solid line). Diffraction of soft x rays ($\lesssim$1.5 keV) will contribute to image blurring at best focus. The dotted line in Fig. 74.28(d) indicates the approximate effect of diffraction on the resolution for an assumed energy of 1.25 keV (worst case, i.e., lowest practical energy to be used). Diffraction is seen to limit the resolution to ~2 μm for such soft x rays. The measured resolution of 3 μm at best focus indicates that the optical system is limited to $\geq$1.5 times the diffraction limit. For comparison the resolution that would have been obtained if 9-mm-thick mirrors had been used is shown in Fig. 74.28(d) as a dot–dashed line. The smaller mirrors clearly provide a more optimum on-axis and off-axis resolution at the expense of solid angle.

The edge response function ε of the microscope (image of the shadow of the edge of a wire) is given by

$$\varepsilon(x)=\int_{-\infty}^{x}\ell(x')dx', \tag{2}$$

where ℓ is the line spread function, which is itself a function of x and y, but assumed to vary slowly. We can make the simplifying assumption that the point spread function (PSF) is given by the product of the line spread functions in the two perpendicular directions x and y. This is a good assumption provided the axes x and y are aligned along the axes of the microscope mirrors, as is the case for all of the images analyzed in this article. The PSF is thus computed from the observed edge response function by differentiation. The result of one such computation from the image of Fig. 74.28(a) near best focus is shown in Fig. 74.29(a). The computed PSF has a full width at half-maximum of 3.0 μm. Figure 74.29(b) shows the modulation transfer function (MTF)

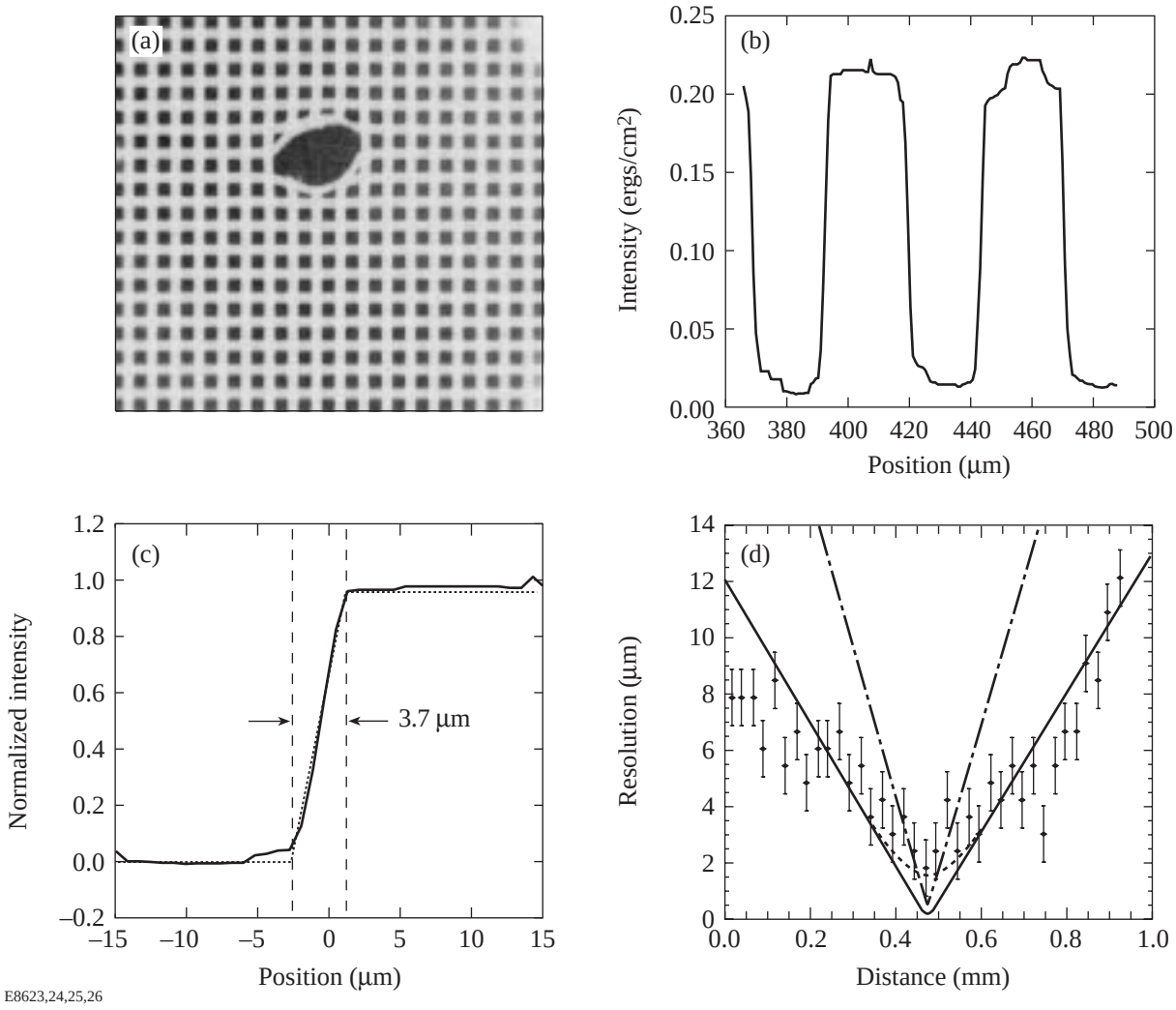

Figure 74.28
Laboratory tests of imaging with the KB microscope. (a) Image of a backlit Cu mesh taken with a cw x-ray source; (b) lineout below hole in grid passing through best focus; (c) enlargement of lineout near best focus; (d) width of the shadow of each wire versus position in the object plane of (a). The solid line is the resolution computed by ray tracing; the dotted line includes the effect of diffraction by 1.25-keV x rays. The dot–dashed line is the resolution computed by ray tracing for 9-mm-thick mirrors (as used in Ref. 12).

$$\mathrm{MTF} = F\left[\mathrm{PSF}(x)\right], \tag{3}$$

computed from the PSF by Fourier transform as a function of position about best focus. The ideal MTF of a pinhole camera with a 10-μm aperture at comparable magnification is shown for comparison.

Framed imaging with the KB microscope is accomplished with a pair of custom microchannel plate (MCP)–based cameras built at the Los Alamos National Laboratory[13] and originally designed to be used in the gated monochromatic x-ray imager[18] (GMXI), which also uses a KB optic for imaging. The GMXI vacuum housing and KB microscope chassis with the uncoated KB microscope optic were used to obtain framed images on the OMEGA target chamber. Each camera consists of a pair of 25-mm-diam MCP's proximity focused to P-11 phosphor-coated fiber-optic faceplates. Two such cameras record the four images of the KB microscope on Kodak TMAX 3200 film. A frame time of ~80 ps results when the cameras are electrically gated. Each camera can be independently triggered, while the separation of the images (~48 mm) results in a time between images on a camera of ~320 ps. Laboratory tests of the framing camera/KB microscope combination were

performed with the cw x-ray source described above, prior to its use on OMEGA. Figure 74.30(a) shows one such image. The resultant MTF is shown in Fig. 74.30(b) and is compared to the MTF's of the KB microscope without a framing camera and the MTF of a 10-μm pinhole at comparable magnification. As is evident, some amount of spatial resolution is lost when using the framing cameras with the KB microscope. The framing camera allows flexibility, however, in choosing the time of the radiograph when not using a short-pulse backlighter.

The energy dependence of the KB optic reflectivity was measured with the same tungsten x-ray source described above using the method described in Dhez *et al.*[19] The spectrum of both the reflected and unreflected x rays were recorded with a AMPTEK XR-100T Si(Li) detector.[20] The reflectivity was computed from the ratio of the two observed spectra and is shown in Fig. 74.31 along with the reflectivity computed from the tabulated values of the atomic scattering factors[21] and assuming a grazing angle of 0.70°. Both the ideal calculated response and the response convolved with the Si(Li) detector energy resolution are shown. The measurements were taken through a path that contained 38 μm of Be, which limited the sensitivity below 1.5 keV. The difference between the measured and computed reflectivities is small and may be due to

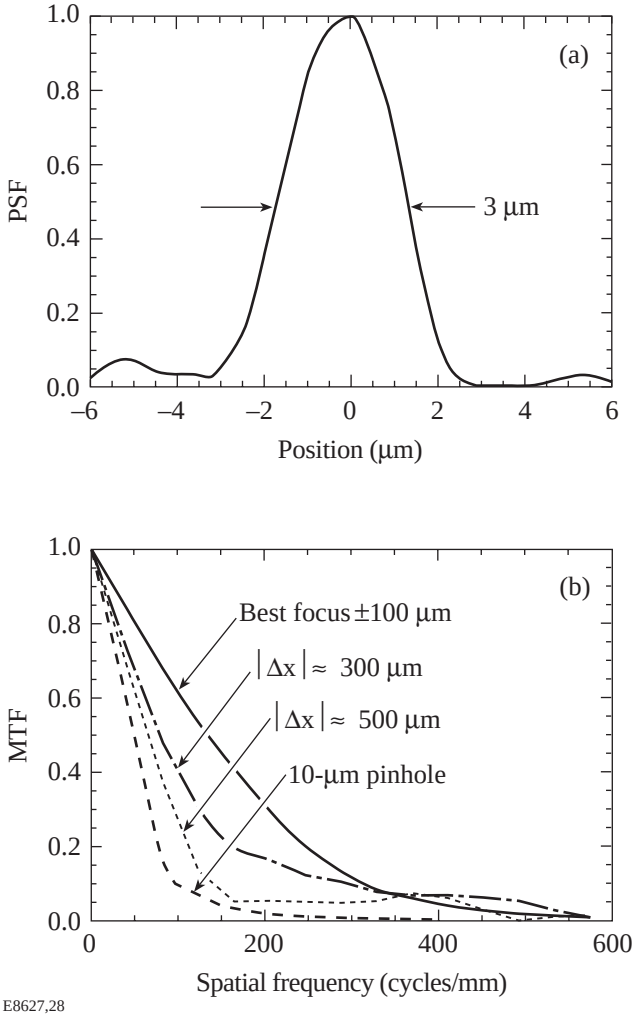

Figure 74.29
The PSF and MTF of the KB microscope recorded with DEF film. (a) The PSF near best focus; (b) the MTF versus position compared to that of a 10-μm pinhole at comparable magnification.

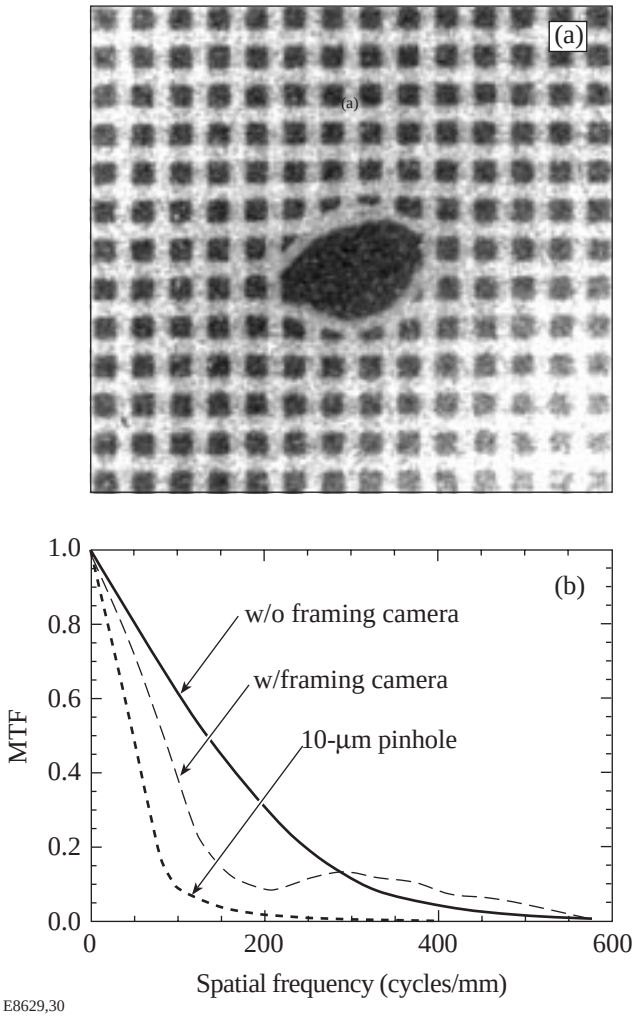

Figure 74.30
Laboratory test of the KB microscope with images recorded by a framing camera. (a) Image of the grid taken with a framing camera and a cw x-ray source; (b) the MTF of the KB microscope with framing camera–recorded images compared to the same obtained without framing cameras. The MTF of a 10-μm-pinhole-camera–based framing camera is also shown for comparison (dotted line).

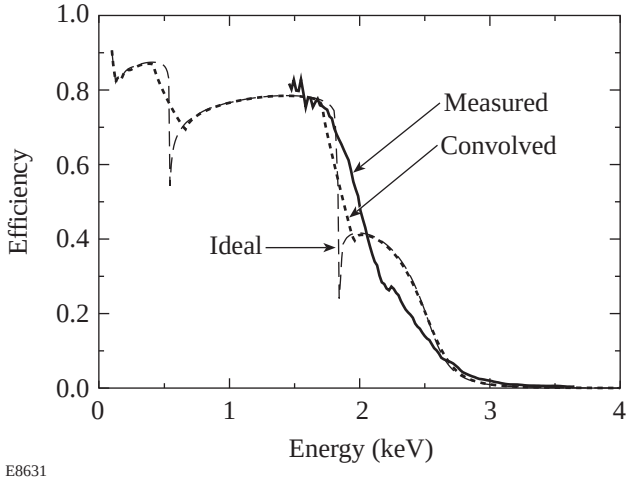

Figure 74.31
The reflectivity of the KB microscope versus energy. The solid line is the measured reflectivity, the dashed line is the reflectivity computed using tabulated values of the atomic scattering constants, and the dotted line includes the convolved response of the Si(Li) detector.

imprecise knowledge of the energy resolution of the Si(Li) detector at the low energies involved. The reflectivity is seen to fall at the Si edge (1.8 keV) and cut off at ~3 keV as expected due to the usual grazing-angle dependence of the x-ray reflectivity.

The choice of uncoated glass as the reflecting surface for planar-foil radiography is further elucidated by the following spectral analysis: A typical backlighter used for these experiments is a uranium foil illuminated at intensities of ~3 × 10^{14} W/cm^2. The spectrum of x rays emitted by such a backlighter[22] is shown in Fig. 74.32(a). Most of the emission comes from the uranium *N*-band (which is unresolved in this measured spectrum) with an additional peak at 3.5 keV due to *M*-band emission. A sensitivity weighted toward the low-energy end of the spectrum (<1.5 keV) is desired since the radiography is to be performed on a plastic (CH) foil. The uncoated-glass optic has a sharp dip in the reflectivity at 1.8 keV followed by a gradual decrease to nearly zero from 2 to 3 keV. The cutoff above 3 keV provides for complete rejection of *M*-band x rays (which would decrease the contrast of the radiography). The response to the U-backlighter spectrum can be further optimized with filtration. Figure 74.32(b) shows the computed efficiency of the KB optic when a 25.4-μm-thick Be plus a 6-μm Al filter is used. Figure 74.32(c) shows the spectral flux density seen at the image plane calculated for 10 J in a 300-μm-diam spot in a 100-ps interval (~1.5 × 10^{14} W/cm^2). This combination of microscope reflectivity and filter transmission is seen to result in a spectrum of x rays in a narrow band from ~1 to ~1.5 keV. The 1/*e* depth of x rays through plastic (such as parylene) in the midpoint of the band (1.25 keV) is ~9 μm. Conversely, a 0.5-μm variation in thickness through the foil would produce a modulation in the x-ray signal of ~5%. The calculated flux density is more than adequate to produce a good exposure on Kodak DEF (as would be the case when using a short-pulse backlighter).

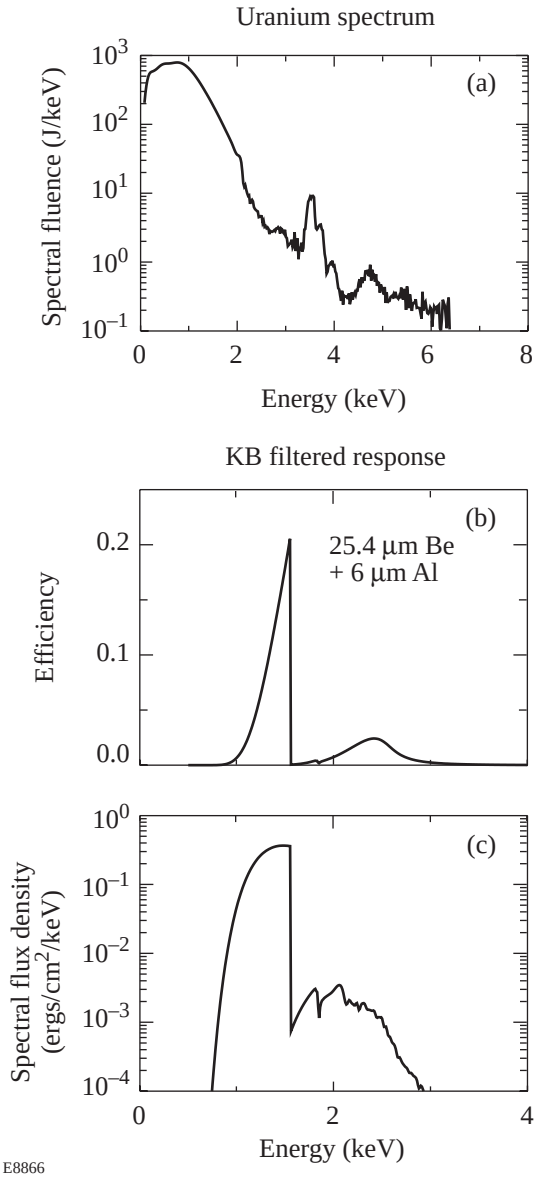

Figure 74.32
The response of the KB microscope to a uranium backlighter. (a) U-backlighter spectrum;[22] (b) the KB microscope response with a 25.4-μm Be plus 6-μm Al filter; (c) spectral flux density at the image plane calculated from the spectrum in (a) and the filter in (b).

Experiments on the OMEGA Laser Facility

Experiments were performed on the OMEGA 60-beam, UV (351-nm) laser system[14] using the soft x-ray KB optic to image laser–plasma x-ray emission. The KB microscope arrangement and the target-illumination method are shown in Fig. 74.33. Targets consisted of test grids and/or driven modulated foils backlit by U foils, illuminated by up to six beams of OMEGA at an intensity of up to 2.5×10^{14} W/cm^2. Figure 74.34 shows a set of such images of backlit grids. [The grids in this case were 25-μm-thick electroetched Ni mesh with a 500/in. pattern (e.g., 50-μm pattern) and 10-μm-square holes.] Grid shots were used to verify the system alignment and provide an *in-situ* measurement of the resolution. Figure 74.34(a) is a DEF-recorded image of a long-pulse (~3-ns) backlit grid, Fig. 74.34(b) is a DEF-recorded image of a short-pulse (~200-ps FWHM Gaussian) backlit grid, and Fig. 74.34(c) is a framing camera–recorded image of a long-pulse backlit grid. Analysis of the images yields MTF's indistinguishable from those shown in Fig. 74.30(b), verifying that the resolution of the microscope is maintained when using a laser–plasma source as a backlighter. Again, spatial resolution of 3 μm is obtained when the radiographs are recorded without the aid of a framing camera.

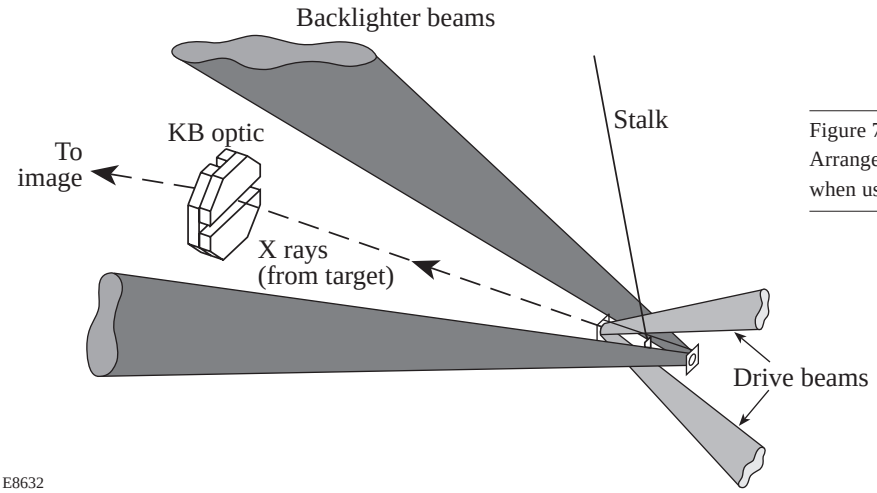

Figure 74.33
Arrangement of KB microscope, target, and beams of OMEGA when used for backlit flat-foil imaging.

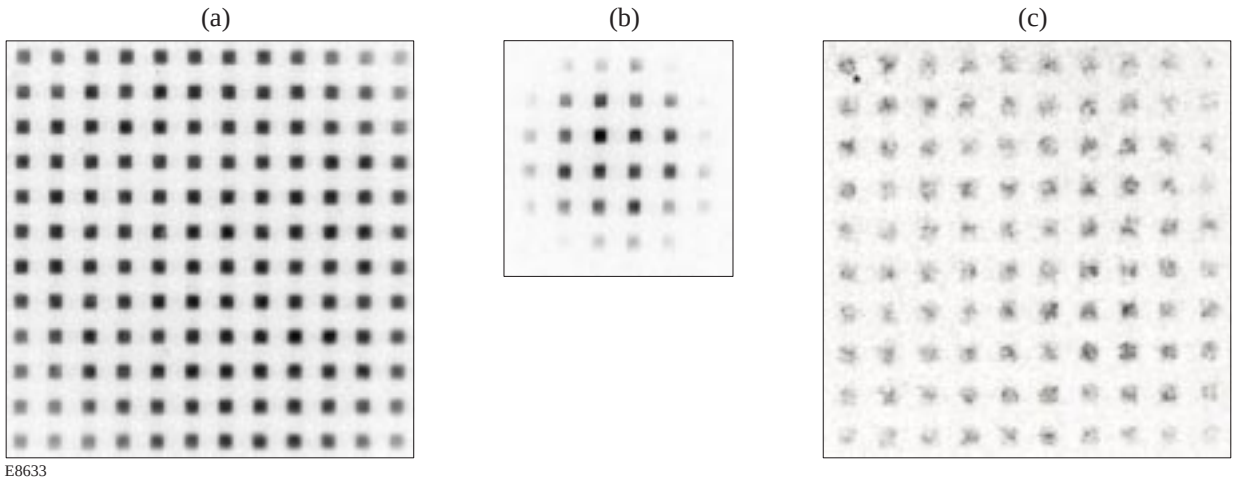

Figure 74.34
Resolution tests performed on the OMEGA laser system. (a) DEF-recorded image of a long-pulse backlit grid; (b) DEF-recorded image of a short-pulse backlit grid; and (c) framing camera–recorded image of a long-pulse backlit grid.

The framing cameras were used to image radiographs of driven perturbed foils. The overall experiments to observe Rayleigh–Taylor (RT) growth are more completely described in Knauer *et al.*[6] Figure 74.35(a) shows a framed image of one such driven foil, which consisted of a 20-μm-thick plastic foil with a 1.0-μm peak-to-valley, 20-μm period modulation on the driven side. The drive intensity was ~2×10^{14} W/cm^2. An intensity-converted lineout taken vertically through the image is shown in Fig. 74.35(b). (The values are deviations from the local average intensity.) An observed variation of ~6% peak-to-valley is evident, which is consistent with early-time (t < 0.5 ns) modulation, assuming the average energy of the x rays producing the modulation is ~1.25 keV. The image shown in Fig. 74.35 serves as an example of the microscope's capabilities.

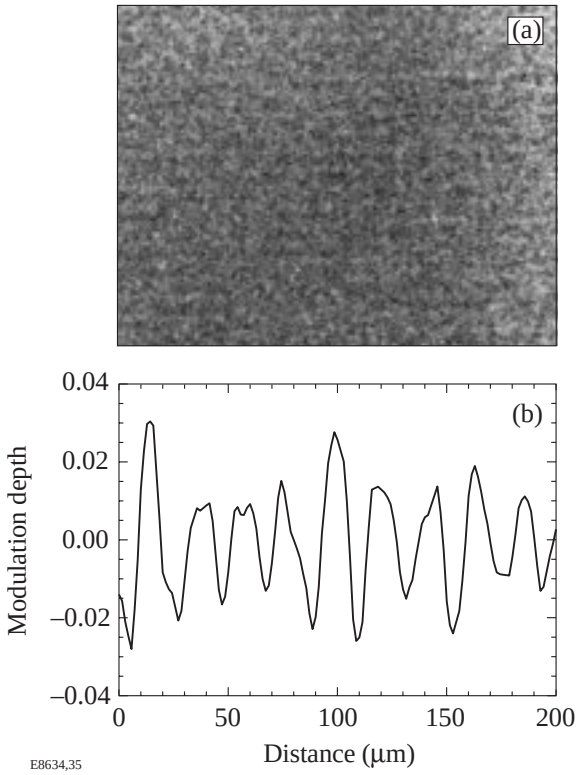

Figure 74.35
Radiograph of driven modulated foil. (a) Framed image of driven foil having an initial modulation depth of 1.0 μm and a 20-μm period; (b) lineout through the image.

Multiple-Beam, Short-Pulse Backlighting

The best possible method for utilizing the high spatial resolution of the KB microscope is to record the radiographs directly with x-ray sensitive film, or with a solid-state device having comparable spatial resolution, as was demonstrated in the preceding section. Since it is necessary to observe the time evolution of the object being radiographed in this instance (i.e., the modulated driven foil), a short-pulse (~100 ps or less) backlighter is required. This can be accomplished on OMEGA with up to six beams, as shown schematically in Fig. 74.36. The short pulses are staggered in time to arrive at the backlighter, spaced by the desired delay, and arranged to backlight the target from separate but nearby directions as seen from the microscope. Since the microscope, as installed in the OMEGA target chamber, is surrounded by six beams, a natural arrangement is for the beams to backlight the driven target in a hexagonal pattern. Tests are currently underway to provide for this experimental configuration on OMEGA.

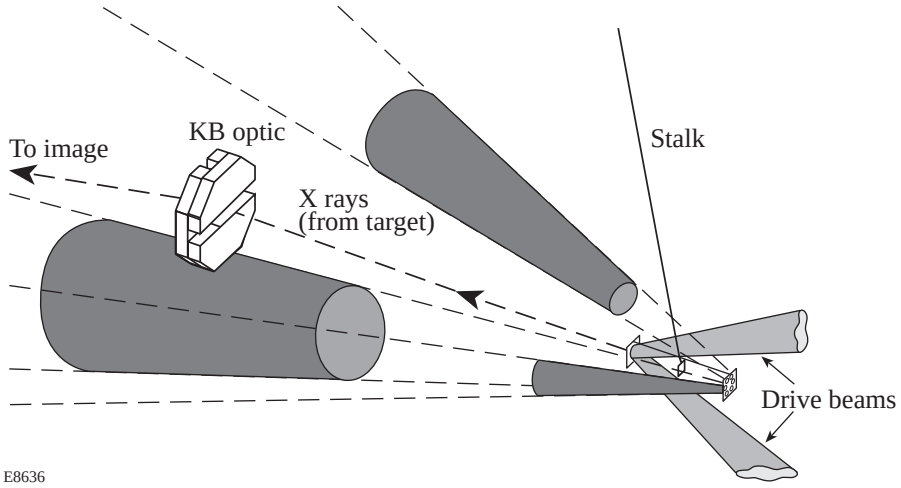

Figure 74.36
Configuration for obtaining multiframe radiographs by multibeam, short-pulse backlighter irradiation.

Conclusions

The KB microscope described in this article has a demonstrated resolution of ~3 μm at optimum focus and a sensitive energy range of ~1 to 3 keV dependent on filtration. When used with a framing camera, the obtainable resolution is degraded to ~7 μm, but with the benefit of ~80-ps time resolution afforded by the cameras. Both high-spatial (~3-μm) and temporal resolution can be obtained by using a multiple-beam, short-pulse backlighter configuration. In conclusion, the KB microscope described here as used in the GMXI is a flexible diagnostic of laser-driven, planar-foil experiments, providing the desired time-resolved, high-spatial-resolution x-ray radiographs.

ACKNOWLEDGMENT

The authors acknowledge the support of the staffs at the Laboratory for Laser Energetics and the Los Alamos National Laborabory. This work was supported by the U.S. Department of Energy Office of Inertial Confinement Fusion under Cooperative Agreement No. DE-FC03-92SF19460, the University of Rochester, and the New York State Energy Research and Development Authority. The support of DOE does not constitute an endorsement by DOE of the views expressed in this article.

REFERENCES

1. J. Grun *et al*., Phys. Rev. Lett. **58**, 2672 (1987).
2. M. Desselberger *et al*., Phys. Rev. Lett. **65**, 2997 (1990).
3. S. G. Glendinning, S. V. Weber, P. Bell, L. B. DaSilva, S. N. Dixit, M. A. Henesian, D. R. Kania, J. D. Kilkenny, H. T. Powell, R. J. Wallace, P. J. Wegner, J. P. Knauer, and C. P. Verdon, Phys. Rev. Lett. **69**, 1201 (1992).
4. K. Shigemori *et al.*, Phys. Rev. Lett. **78**, 250 (1997).
5. S. G. Glendinning, S. N. Dixit, B. A. Hammel, D. H. Kalantar, M. H. Key, J. D. Kilkenny, J. P. Knauer, D. M. Pennington, B. A. Remington, R. J. Wallace, and S. V. Weber, Phys. Rev. Lett. **78**, 3318 (1997).
6. J. P. Knauer, C. P. Verdon, D. D. Meyerhofer, T. R. Boehly, D. K. Bradley, V. A. Smalyuk, D. Ofer, P. W. McKenty, S. G. Glendinning, D. H. Kalantar, R. G. Watt, P. L. Gobby, O. Willi, and R. J. Taylor, in *Laser Interaction and Related Plasma Phenomena*, edited by G. H. Miley and E. M. Campbell (American Institute of Physics, Woodbury, NY, 1997), Vol. 406, pp. 284–293.
7. C. Brown *et al.*, Phys. Plasmas **4**, 1397 (1997).
8. S. G. Glendinning *et al.*, Rev. Sci. Instrum. **63**, 5108 (1992).
9. H. F. Robey, K. S. Budil, and B. A. Remington, Rev. Sci. Instrum. **68**, 792 (1997).
10. B. A. Remington *et al.*, Rev. Sci. Instrum. **63**, 5080 (1992).
11. R. Kodama *et al.*, Opt. Lett. **21**, 1321 (1996).
12. F. J. Marshall and Q. Su, Rev. Sci. Instrum. **66**, 725 (1995).
13. J. A. Oertel, T. Archuleta, C. G. Peterson, and F. J. Marshall, Rev. Sci. Instrum. **68**, 789 (1997).
14. T. R. Boehly, D. L. Brown, R. S. Craxton, R. L. Keck, J. P. Knauer, J. H. Kelly, T. J. Kessler, S. A. Kumpan, S. J. Loucks, S. A. Letzring, F. J. Marshall, R. L. McCrory, S. F. B. Morse, W. Seka, J. M. Soures, and C. P. Verdon, Opt. Commun. **133**, 495 (1997).
15. Sydor Optics, Inc., Rochester, NY.
16. P. Kirkpatrick and A. V. Baez, J. Opt. Soc. Am. **38**, 766 (1948).
17. B. L. Henke *et al.*, J. Opt. Soc. Am. B **3**, 1540 (1986).
18. F. J. Marshall and J. A. Oertel, Rev. Sci. Instrum. **68**, 735 (1997).
19. P. Dhez, H. Duval, and J. C. Malaurent, J. X-Ray Sci. Technol. **3**, 176 (1992).
20. A. C. Huber, J. A. Pantazis, and V. T. Jordanov, Nucl. Instrum. Methods Phys. Res. B **99**, 665 (1995).
21. B. L. Henke, E. M. Gullikson, and J. C. Davis, At. Data Nucl. Data Tables **54**, 181 (1993).
22. S. G. Glendinning *et al*., in *Applications of Laser Plasma Radiation II*, edited by M. C. Richardson and G. A. Kyrala (SPIE, Bellingham, WA, 1995), Vol. 2523, pp. 29–39.